SABA Publishing

Journal of Mathematical Analysis and Modeling
jmam.sabapub.com
ISSN 2709-5924

J Math Anal & Model
(2023)4(3) : 1-25
doi:10.48185/jmam.v4i3.944

An Optimal Control Model for Coffee Berry Disease and Coffee Leaf Rust Co-infection

H.O. NYABERI [a,*], W.N. MUTUKU[b], D.M. MALONZA[c], G.W. GACHIGUA [d], G.O. ALWORAH [e]

[a,b] Department of Mathematics, Kenyatta University, Kenya
[c] Department of Mathematics, South Eastern University of Kenya
[d] Department of Industrial and Engineering Mathematics, The Technical University of Kenya
[e] Department of Plant Pathology, KALRO-Coffee Research Institute, Kenya

• *Received: 04 January 2024* • *Accepted: 27 February 2024* • *Published Online: 20 March 2024*

Abstract

In the 1980s, coffee production in Kenya peaked at an average of 1.7 million bags annually. Since then, this production has declined to the current output of below 0.9 million bags annually. Coffee berry disease (CBD) and Coffee leaf rust (CLR) are some of the causes of this decline. This is due to insufficient knowledge of optimal control strategies for CBD and CLR co-infection. In this research, we derive a system of ODEs from the mathematical model for co-infection of CBD and CLR with control strategies to perform optimal control analysis. An optimal control problem is formulated and solved using Pontryagin's maximum principle. The outcomes of the model's numerical simulations indicate that combining all interventions is the best strategy for slowing the spread of the CBD-CLR co-infection.

Keywords: Coffee Berry Disease, Coffee Leaf Rust, Optimal control, Numerical Simulation.
2010 MSC: 92B05, 93A30, 34D20.

1. Introduction

Coffee is one of the major cash crops in Kenya. According to the Coffee Research Institute of Kenya, coffee is grown in large and small-scale farms, whereby 70% of coffee production is from small-scale farms. The regions where coffee is grown in Kenya are Mt. Kenya, Rift Valley, Nyanza, and Western. These comprise 32 counties out of a total of 47 counties in Kenya [1].

In the 1980s, coffee production in Kenya peaked at an average of 1.7 million bags annually [2]. Since then, this production has declined to the current production of below 0.9 million bags annually due to several factors like diseases and insect pest attacks, nutritional

*Corresponding author: halsonogeto@gmail.com

deficiencies, and management [1]. For instance, Coffee Berry Disease (CBD) and Coffee Leaf Rust (CLR) are some of the diseases that have contributed to the decline of coffee production in Kenya.

Coffee Berry Disease is caused by the fungus *Colletotrichum kahawae*. The first documentation of CBD dates back to 1922 in western Kenya. The disease led to the severe destruction of coffee plantations in the region [3].

Coffee leaf rust (CLR), caused by the fungus *Hemileia vastatrix*, is one of the most common diseases affecting coffee worldwide. It is Kenya's second most serious after CBD [4]. CLR was first discovered in Kenya in 1912 [5]. According to [6], CBD can cause up to 70-80 % of losses and CLR may lead to loss of berries up to 70% and foliage up to 50%.

Mathematical models have been used to study human, animal, and plant disease dynamics, see [7, 8, 9]. A few models have been proposed for studying CBD. For instance, a mathematical model to study the dynamics of CBD by [10]. However, several CLR models have been considered in recent years. Some of these models investigate the factors that affect CLR intensity in several plots in Honduras [11], and the connection between the local and regional dynamics of the CLR model [12].

Vandermeer *et al*.[13] used an SI epidemiological model of the host to represent the CLR dynamics on a coffee farm in Chiapas. Djuikem *et al*. [14] constructed and analyzed a PDE model to describe CLR transmission in a coffee farm during wet and dry seasons and its behavior over time. Djuikem *et al.* [15] proposed a model of the coffee leaf rust (CLR) with optimal control.

The co-infection concept has been captured in several mathematical models of infectious diseases; see, for example, HIV-Tuberculosis co-infection ([16], [17]), malaria and cholera [18], pneumonia and typhoid [19]. Co-infection phenomena, like human diseases, are expected to alter the course of infection in co-infected plants [20]. However, co-infection in plants such as coffee is a topic that hasn't gotten much attention. Thus, this research seeks to study the optimal control of the co-infection of CBD and CLR.

2. Model Formulation

This study builds upon the model presented in the study [10], which discussed the dynamics of CBD. To investigate the dynamics of CBD-CLR co-infection, we divided the coffee plants in the plantation into eight classes at any time t, namely, the susceptible coffee plants $S(t)$, coffee plants exposed to *Colletotrichum kahawae* $E_k(t)$, plants exposed to *Hemileia vastatrix* $E_v(t)$, co-exposed coffee plants $E_{kv}(t)$, the CBD infected coffee plants $I_k(t)$, the CLR infected coffee plants $I_v(t)$, the co-infected coffee plants $I_{kv}(t)$ and recovered coffee plants $R(t)$ such that the total number of coffee plants is given by $N(t) = S(t) + E_k(t) + I_k(t) + E_v(t) + I_v(t) + E_{kv}(t) + I_{kv}(t) + R(t)$. The number of *Colletotrichum kahawae* and *Hemileia vastatrix* pathogens in the plantation at any time t is $P_k(t)$ and $P_v(t)$ respectively. The model is schematically described in the Figure 1

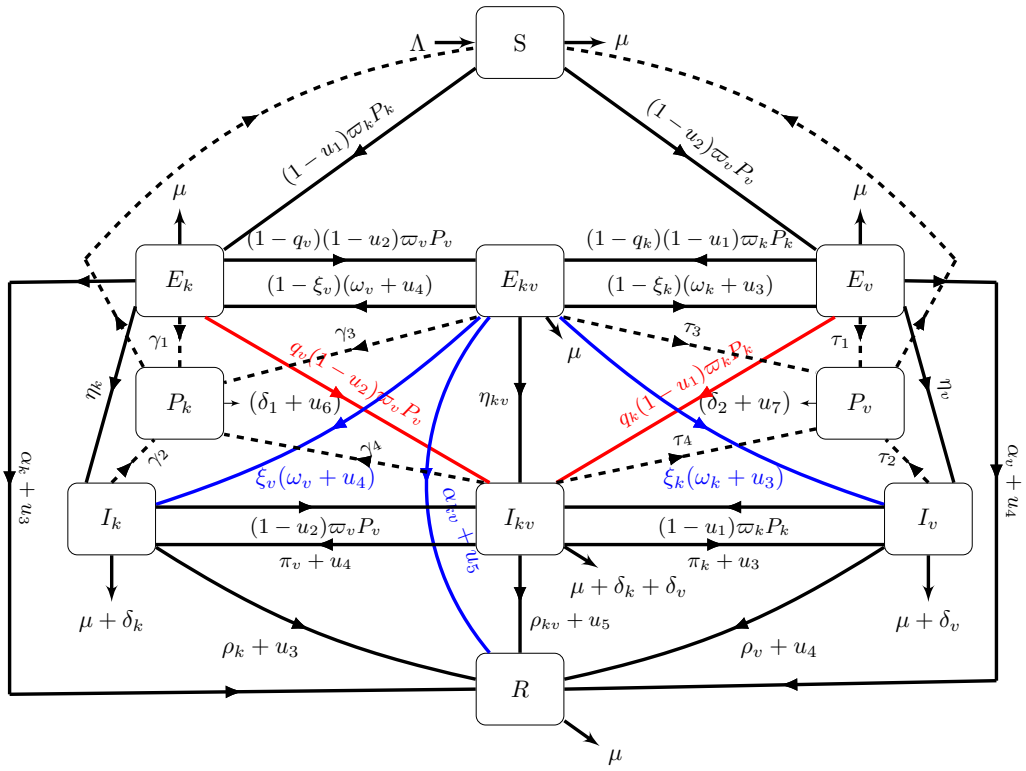

Figure 1: Flow chart of epidemic coffee plants

From Figure 1 we derive the following equations:

$$
\begin{aligned}
\frac{dS}{dt} &= \Lambda-(1-u_1)\varpi_k P_k S-(1-u_2)\varpi_v P_v S-\mu S,\\
\frac{dE_k}{dt} &= (1-u_1)\varpi_k P_k S+(1-\xi_v)(\omega_v+u_4)E_{kv}-(\alpha_k+u_3)E_k-((1-u_2)\varpi_v P_v+\mu+\eta_k)E_k,\\
\frac{dE_v}{dt} &= (1-u_2)\varpi_v P_v S+(1-\xi_k)(\omega_k+u_3)E_{kv}-(\alpha_v+u_4)E_v-((1-u_1)\varpi_k P_k+\mu+\eta_v)E_v,\\
\frac{dE_{kv}}{dt} &= (1-u_2)(1-q_v)\varpi_v P_v E_k+(1-u_1)(1-q_k)\varpi_k P_k E_v-(\omega_k+u_3)E_{kv}-(\omega_v+u_4)E_{kv}\\
&\quad -(\alpha_{kv}+u_5)E_{kv}-(\mu+\eta_{kv})E_{kv},\\
\frac{dI_k}{dt} &= \eta_k E_k+\xi_v(\omega_v+u_4)E_{kv}+(\pi_v+u_4)I_{kv}-(1-u_2)\varpi_v P_v I_k-(\rho_k+u_3)I_k-(\mu+\delta_k)I_k,\\
\frac{dI_v}{dt} &= \eta_v E_v+\xi_k(\omega_k+u_3)E_{kv}+(\pi_k+u_3)I_{kv}-(1-u_1)\varpi_k P_k I_v-(\rho_v+u_4)I_v-(\mu+\delta_v)I_v,\\
\frac{dI_{kv}}{dt} &= (1-u_2)q_v\varpi_v P_v E_k+(1-u_1)q_k\varpi_k P_k E_v+(1-u_1)\varpi_k P_k I_v+(1-u_2)\varpi_v P_v I_k+\eta_{kv}E_{kv}\\
&\quad -(\pi_k+u_3)I_{kv}-(\pi_v+u_4)I_{kv}-(\rho_{kv}+u_5)I_{kv}-(\mu+\delta_k+\delta_v)I_{kv},\\
\frac{dP_k}{dt} &= \gamma_1 E_k+\gamma_2 I_k+\gamma_3 E_{kv}+\gamma_4 I_{kv}-(\delta_1+u_6)P_k,
\end{aligned}
$$

$$\begin{aligned}
\frac{dP_\nu}{dt} &= \tau_1 E_\nu + \tau_2 I_\nu + \tau_3 E_{k\nu} + \tau_4 I_{k\nu} - (\delta_2 + u_7)P_\nu, \\
\frac{dR}{dt} &= (\alpha_k + u_3)E_k + (\alpha_\nu + u_4)E_\nu + (\alpha_{k\nu} + u_5)E_{k\nu} + (\rho_k + u_3)I_k + (\rho_\nu + u_4)I_\nu + (\rho_{k\nu} + u_5)I_{k\nu} \\
&\quad -\mu R,
\end{aligned} \tag{2.1}$$

Where Λ is the recruitment rate of susceptible coffee trees through continuous planting, μ is the natural death rate of coffee trees, ϖ_k is the rate at which coffee trees are exposed to the coffee berry disease through contact with *Colletotrichum kahawae*, ϖ_ν is the rate at which coffee trees are exposed to coffee leaf rust through contact with *Hemileia vastatrix*, $0 < q_k < 1$, $0 < q_\nu < 1$, $0 < \xi_k < 1$ and $0 < \xi_\nu < 1$ are constants of proportion, η_k is the rate at which coffee trees in E_k progress to I_k, α_k is the rate at which coffee trees in E_k recover, η_ν is the rate at which coffee trees in E_ν progress to I_ν, α_ν is the rate at which coffee trees in E_ν recover, $\eta_{k\nu}$ is the rate at which coffee trees in $E_{k\nu}$ progress to $I_{k\nu}$, $\alpha_{k\nu}$ is the rate at which coffee trees in $E_{k\nu}$ recover from both CBD and CLR, ω_ν is CLR recovery rate of coffee trees in $E_{k\nu}$, ω_k is CBD recovery rate of coffee trees in $E_{k\nu}$, ρ_k is the rate at which coffee trees in I_k recover, ρ_ν is the rate at which coffee trees in I_ν recover, $\rho_{k\nu}$ is the rate at which coffee trees in $I_{k\nu}$ recover from both CBD and CLR, π_ν is CLR recovery rate of coffee trees in $I_{k\nu}$, π_k is CBD recovery rate of coffee trees in $I_{k\nu}$, δ_k is CBD-induced death rate, δ_ν is CLR-induced death rate , γ_1, γ_2, γ_3 and γ_4 are the rates at which coffee trees in $E_k(t)$, $I_k(t)$, $E_{k\nu}(t)$ and $I_{k\nu}(t)$ contribute to the increase of P_k pathogens in the environment respectively, τ_1, τ_2, τ_3 and τ_4 are the rates at which coffee trees in $E_\nu(t)$, $I_\nu(t)$, $E_{k\nu}(t)$ and $I_{k\nu}(t)$ contribute to the increase of P_ν pathogens in the environment respectively, and δ_1 and δ_2 are the decay rates of the pathogens in P_k and P_ν classes respectively. Also, $(u_i(t),\ i = 1, 2, \cdots, 7)$ are time-dependent control measures that reduce the rate of CBD and CLR infection, and they are defined as:

(i) u_1— prevention of CBD infection by use of cultural measures (pruning and weeding) and planting resistant coffee varieties such as K7 (k gene), Hibrido de Timor (Ck-1 or T gene) and Rume Sudan (R and K genes)

(ii) u_2— prevention of CLR infection by spraying copper oxychloride, using resistant/tolerant plant cultivars from suggested nurseries, and cultural measures including appropriate pruning and weeding.

(iii) u_3— Treatment of CBD-infected coffee plants by applying copper-based fungicides such as Nordox 75% EC

(iv) u_4— Treatment of CLR-infected coffee plants by spraying For the management of coffee leaf rust, a tank mixture of copper (5 kg of 50% weightable powder copper oxychloride) and a half-rate organic fungicide (for example, 2 kg of 75% weightable powder chlorothalonil) is also effective.

(v) u_5— Treatment of CBD-CLR Co-infected coffee plants by spraying Tebuconazole

(vi) u_6— Elimination of *Colletotrichum kahawae* pathogens by using bio-control agents such as *Pseudomonas spinosa* ECk-17, *B. mycoides* ECk-06 and *Bacillus megaterium* ECk-05

(vii) u_7 Elimination of *Hemileia vastatrix* pathogens by use of suspensions of *Bacillus* species as a biocontrol

3. Basic Properties of the model

We discuss the Positivity and Boundedness of the solutions of the model.

3.1. Positivity of the solutions of the model

Lemma 3.1. *Let* $S_0 > 0$, $E_{k0} \geqslant 0$,$E_{v0} \geqslant 0$, $E_{kv0} \geqslant 0$,$I_{k0} \geqslant 0$, $I_{v0} \geqslant 0$, $I_{kv0} \geqslant 0$, $P_{k0} \geqslant 0$, $P_{v0} \geqslant 0$, *and* $R_0 \geqslant 0$ *be the initial conditions of the system (2.1) then the solutions* S, E_k,E_v, E_{kv},I_k, I_v, I_{kv}, P_k, P_v, *and* R *are non-negative* $\forall\ t > 0$.

Proof. Considering the system (2.1), the maximum endemic period, T, is determined by $T = \sup\{t > 0 \mid S(\tau) > 0,\ E_k(\tau) \geqslant 0,\ E_v(\tau) \geqslant 0,\ E_{kv}(\tau) \geqslant 0,\ I_k(\tau) \geqslant 0,\ I_v(\tau) \geqslant 0,\ I_{kv} \geqslant 0,\ P_k(\tau) \geqslant 0,\ P_v \geqslant 0,\ R(\tau) \geqslant 0\ \ \forall\tau\ \in\ [0,\ t]\}$.
Taking $S_0 > 0$, $E_{k0} \geqslant 0$, $E_{v0} \geqslant 0$, $E_{kv0} \geqslant 0$,$I_{k0} \geqslant 0$, $I_{v0} \geqslant 0$, $I_{kv0} \geqslant 0$, $P_{k0} \geqslant 0$, $P_{v0} \geqslant 0$, and $R_0 \geqslant 0$, let us express the first equation of the system (2.1) as

$$\frac{dS}{dt} + ((1-u_1)\varpi_k P_k + (1-u_2)\varpi_v P_v + \mu)S = \Lambda. \tag{3.1}$$

Multiplying both sides of equation (3.1) by the integrating factor, we obtain

$$\begin{aligned}\frac{d}{dt}\left(S(t)\exp\left[\int_0^T((1-u_1)\varpi_k P_k + (1-u_2)\varpi_v P_v + \mu)(s)ds\right]\right)\\ = \Lambda\exp\left(\int_0^T((1-u_1)\varpi_k P_k + (1-u_2)\varpi_v P_v + \mu)(s)ds\right).\end{aligned} \tag{3.2}$$

Equation (3.2)'s both sides are integrated from 0 to T to produce the following result.

$$\begin{aligned}S(T) = \exp\left[-\int_0^T((1-u_1)\varpi_k P_k + (1-u_2)\varpi_v P_v + \mu)(s)ds\right]\bullet\\ \left\{S_0 + \int_0^T \Lambda\exp\left[\int_0^{\tilde{T}}((1-u_1)\varpi_k P_k + (1-u_2)\varpi_v P_v + \mu)(\tau)d\tau\right]d\tilde{T}\right\}.\end{aligned} \tag{3.3}$$

Thus $S(t) > 0\ \forall\ t > 0$.
From the second equation of the system (2.1), we have

$$\frac{dE_k}{dt} \geqslant -(\alpha_k + u_3 + (1-u_2)\varpi_v P_v + \mu + \eta_k)E_k. \tag{3.4}$$

Solving equation (3.4) yields

$$E_k \geqslant E_{k0} \exp\left\{-\left[(\alpha_k + u_3 + \mu + \eta_k)T + \int_0^T (1-u_2)\varpi_v P_v(s)ds\right]\right\} \geqslant 0. \tag{3.5}$$

Using the same methodology to prove the next eight equations, we arrive at
$E_v(t) \geqslant 0$, $E_{kv}(t) \geqslant 0$,$I_k(t) \geqslant 0$, $I_v(t) \geqslant 0$, $I_{kv}(t) \geqslant 0$, $P_k(t) \geqslant 0$, $P_v(t) \geqslant 0$ $R(t) \geqslant 0$.
As a result, every solution of the system (2.1) is positive $\forall\ t > 0$. □

3.2. Boundedness of the solutions of the model

This section demonstrates that every feasible solution is uniformly bounded in a proper subset $\mathscr{D}$.

Lemma 3.2. *Let the initial conditions of system (2.1) be non-negative in* $\mathbb{R}^{10}_+$,
$\mathscr{D}_N = \left\{(S,\ E_k,\ E_v,\ E_{kv},\ I_k,\ I_v,\ I_{kv},\ R) \in \mathbb{R}^8_+ : N(t) \leqslant \frac{\Lambda}{\mu}\right\}$,
$\mathscr{D}_{P_k} = \left\{P_k \in \mathbb{R}^1_+ : P_k(t) \leqslant \frac{\Lambda(\gamma_1+\gamma_2+\gamma_3+\gamma_4)}{\mu\delta_1}\right\}$ *and* $\mathscr{D}_{P_v} = \left\{P_v \in \mathbb{R}^1_+ : P_v(t) \leqslant \frac{\Lambda(\tau_1+\tau_2+\tau_3+\tau_4)}{\mu\delta_2}\right\}$
then the set $\mathscr{D} = \mathscr{D}_N \cup \mathscr{D}_{P_k} \cup \mathscr{D}_{P_v} \subset \mathbb{R}^8_+ \times \mathbb{R}^1_+ \times \mathbb{R}^1_+$ *is positively invariant.*

Proof. In this lemma, we are required to show that $\mathscr{D}_N$, $\mathscr{D}_{P_k}$ and $\mathscr{D}_{P_v}$ are positively invariant. To begin, we add the system (2.1)'s first seven equations together with its final equation to arrive at

$$\frac{dN}{dt} = \Lambda - \mu N - (\delta_k I_k + \delta_v I_v + \delta_k I_{kv} + \delta_v I_{kv}). \tag{3.6}$$

In the absence of the CBD and CLR, we have

$$\frac{dN}{dt} \leqslant \Lambda - \mu N. \tag{3.7}$$

Solving equation (3.7) for N, we arrive

$$N(t) \leqslant \frac{\Lambda}{\mu} + \left\{N_0 - \frac{\Lambda}{\mu}\right\} e^{-\mu t}. \tag{3.8}$$

Hence

$$N(t) \leqslant \frac{\Lambda}{\mu} \text{ as } t \to \infty.$$

Therefore the feasible region for the coffee plant population in the system (2.1) is defined by

$$\mathscr{D}_N = \left\{(S,\ E_k,\ E_v,\ E_{kv},\ I_k,\ I_v,\ I_{kv},\ R) \in \mathbb{R}^8_+ : N(t) \leqslant \frac{\Lambda}{\mu}\right\}.$$

In view of the eighth equation of system (2.1), the equation for *Colletotrichum kahawae* pathogens,

$\frac{dP_k}{dt} = \gamma_1 E_k + \gamma_2 I_k + \gamma_3 E_{kv} + \gamma_4 I_{kv} - \delta_1 P_k$,

We rewrite it as

$$\frac{dP_k}{dt} \leqslant \frac{\Lambda(\gamma_1+\gamma_2+\gamma_3+\gamma_4)}{\mu} - \delta_1 P_k. \tag{3.9}$$

Solving equation (3.9), we get

$$P_k(t) \leqslant \frac{\Lambda(\gamma_1+\gamma_2+\gamma_3+\gamma_4}{\mu\delta_1} + \left(P_{k0} - \frac{\Lambda(\gamma_1+\gamma_2+\gamma_3+\gamma_4)}{\mu\delta_1}\right) e^{-\delta_1 t} \tag{3.10}$$

Hence

$$P_k(t) \leqslant \frac{\Lambda(\gamma_1+\gamma_2+\gamma_3+\gamma_4)}{\mu\delta_1} \text{ as } t \to \infty.$$

Therefore, the feasible region for *Colletotrichum kahawae* pathogens is given by

$$\mathscr{D}_{P_k} = \left\{ P_k \in \mathbb{R}^1_+ : P_k(t) \leqslant \frac{\Lambda(\gamma_1+\gamma_2+\gamma_3+\gamma_4)}{\mu\delta_1} \right\}.$$

From the ninth equation of system (2.1), the equation for *Hemileia vastatrix* pathogens,
$\frac{dP_v}{dt} = \tau_1 E_v + \tau_2 I_v + \tau_3 E_{kv} + \tau_4 I_{kv} - \delta_2 P_v$,
we have

$$\frac{dP_v}{dt} \leqslant \frac{\Lambda(\tau_1+\tau_2+\tau_3+\tau_4)}{\mu} - \delta_2 P_v. \tag{3.11}$$

Upon solving equation (3.11) for $P_v(t)$, we obtain

$$P_v(t) \leqslant \frac{\Lambda(\tau_1+\tau_2+\tau_3+\tau_4)}{\mu\delta_1} + \left(P_{v0} - \frac{\Lambda(\tau_1+\tau_2+\tau_3+\tau_4)}{\mu\delta_2}\right) e^{-\delta_2 t}. \tag{3.12}$$

Therefore

$$P_v(t) \leqslant \frac{\Lambda(\tau_1+\tau_2+\tau_3+\tau_4)}{\mu\delta_2} \text{ as } t \to \infty.$$

Hence the feasible region for *Hemileia vastatrix* pathogens is given by

$$\mathscr{D}_{P_v} = \left\{ P_v \in \mathbb{R}^1_+ : P_v(t) \leqslant \frac{\Lambda(\tau_1+\tau_2+\tau_3+\tau_4)}{\mu\delta_2} \right\}.$$

As a result, the feasible region defined by the set $\mathscr{D} = \mathscr{D}_N \cup \mathscr{D}_{P_k} \cup \mathscr{D}_{P_k} \subset \mathbb{R}^8_+ \times \mathbb{R}^1_+ \times \mathbb{R}^1_+$ is positively invariant. □

Since all the system (2.1)'s solutions with non-negative initial conditions are non-negative $\forall\, t > 0$ and $\mathscr{D}$ is positively invariant, which implies that every feasible solution is uniformly bounded in a proper subset $\mathscr{D}$, it follows that the system is appropriate for the study of the optimal control analysis of CBD-CLR co-infection.

4. Optimal control problem

The model's objective is to minimize the number of infections and control costs associated with each control. The objective function to be minimized is formulated as follows:

$$\left.\begin{aligned}\mathcal{J} = \min_{u_1,u_2,u_3,u_4,u_5,u_6,u_7} \int_0^T [&b_1E_k(t) + b_2E_v(t) + b_3E_{kv}(t) + b_4I_k(t) + b_5I_v(t)\\ &+ b_6I_{kv}(t) + b_7P_k(t) + b_8P_v(t) + \frac{1}{2}\sum_{i=1}^{7} v_i u_i^2]dt\end{aligned}\right\} \tag{4.1}$$

Subject to the differential equations in the system (2.1). T is the intervention period. The coefficients b_1, b_2, b_3, b_4, b_5, b_6, b_7, and b_8 are the costs associated with minimizing plants exposed to *Colletotrichum kahawae* (the infected coffee plants which have not showed symptoms) $E_k(t)$, plants exposed to *Hemileia vastatrix* $E_v(t)$, co-exposed plants E_{kv}, the CBD infected coffee plants $I_k(t)$, the CLR infected coffee plants $I_v(t)$, the co-infected plants $I_{kv}(t)$, *Colletotrichum kahawae* pathogens $P_k(t)$ and *Hemileia vastatrix* pathogens $P_v(t)$, respectively. On the other hand, the parameters v_1, v_2, v_3, v_4, v_5, v_6 and v_7 are the costs weights associated with the controls u_1, u_2, u_3, u_4, u_5, u_6, u_7 respectively. Our goal is optimal controls $(u_1^*, u_2^*, u_3^*, u_4^*, u_5^*, u_6^*, u_7^*)$ such that

$$\mathcal{J}(u_1^*, u_2^*, u_3^*, u_4^*, u_5^*, u_6^*, u_7^*) = \min\{\mathcal{J}(u_1, u_2, u_3, u_4, u_5, u_6, u_7) | u_1, u_2, u_3, u_4, u_5, u_6, u_7 \in U\},$$

where the control set $U = \{(u_1(t), u_2(t), u_3(t), u_4(t), u_5(t), u_6(t), u_7(t)) \mid 0 \leqslant u_i \leqslant 1,\ i = 1, 2, \cdots, 7;\ t \in [0, T]\}$ is Lebesgue measurable.

5. The Hamiltonian and Optimality System

We use Pontryagin's Maximum Principle [21] to define the Hamiltonian ($\mathcal{H}$) as:

$$\left.\begin{aligned}\mathcal{H} =&b_1E_k(t) + b_2E_v(t) + b_3E_{kv}(t) + b_4I_k(t) + b_5I_v(t) + b_6I_{kv}(t) + b_7P_k(t)\\ &+ b_8P_v(t) + \frac{1}{2}v_1u_1^2 + \frac{1}{2}v_2u_2^2 + \frac{1}{2}v_3u_3^2 + \frac{1}{2}v_4u_4^2 + \frac{1}{2}v_5u_5^2 + \frac{1}{2}v_6u_6^2 + \frac{1}{2}v_7u_7^2\\ &+ M_1\frac{dS}{dt} + M_2\frac{dE_k}{dt} + M_3\frac{dE_v}{dt} + M_4\frac{dE_{kv}}{dt} + M_5\frac{dI_k}{dt} + M_6\frac{dI_k}{dt} + M_7\frac{dI_{kv}}{dt}\\ &+ M_8\frac{dP_k}{dt} + M_9\frac{dP_v}{dt} + M_{10}\frac{dR}{dt}\end{aligned}\right\}, \tag{5.1}$$

Where M_1, M_2, M_3, M_4, M_5, M_6, M_7, M_8, M_9 and M_{10} are adjoint or co-state variables corresponding to the state variables S, E_k, E_v, E_{kv}, I_k, I_v, I_{kv}, P_k, P_v and R,

respectively. Using system (2.1), we can rewrite equation (5.1) as

$$\begin{aligned}
\mathcal{H} =& b_1 E_k(t) + b_2 E_v(t) + b_3 E_{kv}(t) + b_4 I_k(t) + b_5 I_v(t) + b_6 I_{kv}(t) + b_7 P_k(t) + b_8 P_v(t) \\
&+ \frac{1}{2}\nu_1 u_1^2 + \frac{1}{2}\nu_2 u_2^2 + \frac{1}{2}\nu_3 u_3^2 + \frac{1}{2}\nu_4 u_4^2 + \frac{1}{2}\nu_5 u_5^2 + \frac{1}{2}\nu_6 u_6^2 + \frac{1}{2}\nu_7 u_7^2 \\
&+ M_1\{\Lambda - (1-u_1)\varpi_k P_k S - (1-u_2)\varpi_v P_v S - \mu S\} \\
&+ M_2\{(1-u_1)\varpi_k P_k S + (1-\xi_v)(\omega_v + u_4)E_{kv} - (\alpha_k + u_3)E_k - ((1-u_2)\varpi_v P_v + \mu + \eta_k)E_k\} \\
&+ M_3\{(1-u_2)\varpi_v P_v S + (1-\xi_k)(\omega_k + u_3)E_{kv} - (\alpha_v + u_4)E_v - ((1-u_1)\varpi_k P_k + \mu + \eta_v)E_v\} \\
&+ M_4\{(1-u_2)(1-q_v)\varpi_v P_v E_k + (1-u_1)(1-q_k)\varpi_k P_k E_v - (\omega_k + u_3)E_{kv} - (\omega_v + u_4)E_{kv} \\
&- (\alpha_{kv} + u_5)E_{kv} - (\mu + \eta_{kv})E_{kv}\} \\
&+ M_5\{\eta_k E_k + \xi_v(\omega_v + u_4)E_{kv} + (\pi_v + u_4)I_{kv} - (1-u_2)\varpi_v P_v I_k - (\rho_k + u_3)I_k - (\mu + \delta_k)I_k\} \\
&+ M_6\{\eta_v E_v + \xi_k(\omega_k + u_3)E_{kv} + (\pi_k + u_3)I_{kv} - (1-u_1)\varpi_k P_k I_v - (\rho_v + u_4)I_v - (\mu + \delta_v)I_v\} \\
&+ M_7\{(1-u_2)q_v\varpi_v P_v E_k + (1-u_1)q_k\varpi_k P_k E_v + (1-u_1)\varpi_k P_k I_v + (1-u_2)\varpi_v P_v I_k + \eta_{kv}E_{kv} \\
&- (\pi_k + u_3)I_{kv} - (\pi_v + u_4)I_{kv} - (\rho_{kv} + u_5)I_{kv} - (\mu + \delta_k + \delta_v)I_{kv}\} \\
&+ M_8\{\gamma_1 E_k + \gamma_2 I_k + \gamma_3 E_{kv} + \gamma_4 I_{kv} - (\delta_1 + u_6)P_k\} \\
&+ M_9\{\tau a u_1 E_v + \tau_2 I_v + \tau_3 E_{kv} + \tau_4 I_{kv} - (\delta_2 + u_7)P_v\} \\
&+ M_{10}\{(\alpha_k + u_3)E_k + (\alpha_v + u_4)E_v + (\alpha_{kv} + u_5)E_{kv} + (\rho_k + u_3)I_k + (\rho_v + u_4)I_v \\
&+ (\rho_{kv} + u_5)I_{kv} - \mu R\}. \qquad (5.2)
\end{aligned}$$

Theorem 5.1. *There exist an optimal control set* $\{u_1^*,\ u_2^*,\ u_3^*,\ u_4^*,\ u_5^*,\ u_6^*,\ u_7^*\}$ *that minimizes* $\mathcal{J}$ *over* $\mathcal{U}$ *defined by the equations*

$$\begin{aligned}
u_1^* &= \max\{0, \min\{1, \bar{u}_1\}\}, \\
u_2^* &= \max\{0, \min\{1, \bar{u}_2\}\}, \\
u_3^* &= \max\{0, \min\{1, \bar{u}_3\}\}, \\
u_4^* &= \max\{0, \min\{1, \bar{u}_4\}\}, \\
u_5^* &= \max\{0, \min\{1, \bar{u}_5\}\}, \\
u_6^* &= \max\{0, \min\{1, \bar{u}_6\}\}, \\
u_7^* &= \max\{0, \min\{1, \bar{u}_7\}\},
\end{aligned}$$

where

$$\begin{aligned}
\bar{u}_1 &= \frac{\varpi_k P_k(-SM_1 + SM_2 - E_\nu M_3 + (1-q_k)E_\nu M_4 - I_\nu M_6 + q_k E_\nu M_7 + I_\nu M_7)}{\nu_1},\\
\bar{u}_2 &= \frac{\varpi_\nu P_\nu(-SM_1 + SM_3 - E_k M_2 + (1-q_\nu)E_k M_4 - I_k M_5 + q_\nu E_k M_7 + I_k M_7)}{\nu_2},\\
\bar{u}_3 &= \frac{E_k M_2 - (1-\xi_k)E_{k\nu} M_3 + E_{k\nu} M_4 + I_k M_5 - \xi_k E_{k\nu} M_6 - I_{k\nu} M_6 + I_{k\nu} M_7 - E_k M_{10} - I_k M_{10}}{\nu_3},\\
\bar{u}_4 &= \frac{E_\nu M_3 - (1-\xi_\nu)E_{k\nu} M_2 + E_{k\nu} M_4 - \xi_\nu E_{k\nu} M_5 + I_\nu M_6 - I_{k\nu} M_5 + I_{k\nu} M_7 - E_\nu M_{10} - I_\nu M_{10}}{\nu_4},\\
\bar{u}_5 &= \frac{E_{k\nu} M_4 - E_{k\nu} M_{10} + I_{k\nu} M_7 - I_{k\nu} M_{10}}{\nu_5},\\
\bar{u}_6 &= \frac{P_k M_8}{\nu_6},\\
\bar{u}_7 &= \frac{P_\nu M_9}{\nu_7},
\end{aligned}$$

and the adjoint variables $M_1,\ M_2, \cdots,\ M_{10}$ *satisfying:*

$$\begin{aligned}
\frac{dM_1}{dt} &= (1-u_1)\varpi_k P_k M_1 + (1-u_2)\varpi_\nu P_\nu M_1 + \mu M_1 - (1-u_1)\varpi_k P_k M_2 - (1-u_2)\varpi_\nu P_\nu M_3,\\
\frac{dM_2}{dt} &= -b_1 + (\alpha_k + u_3)M_2 + ((1-u_2)\varpi_\nu P_\nu + \mu + \eta_k)M_2 - (1-u_2)(1-q_\nu)\varpi_\nu P_\nu M_4 - \eta_k M_5\\
&\quad -(1-u_2)q_\nu \varpi_\nu P_\nu M_7 - \gamma_1 M_8 - (\alpha_k + u_3)M_{10},\\
\frac{dM_3}{dt} &= -b_2 + (\alpha_\nu + u_4)M_3 + ((1-u_1)\varpi_k P_k + \mu + \eta_\nu)M_3 - (1-u_1)(1-q_k)\varpi_k P_k M_4 - \eta_\nu M_6\\
&\quad -(1-u_1)q_k \varpi_k P_k M_7 - \tau_1 M_9 - (\alpha_\nu + u_4)M_{10},\\
\frac{dM_4}{dt} &= -b_3 - (1-\xi_\nu)(\omega_\nu + u_4)M_2 - (1-\xi_k)(\omega_k + u_3)M_3 + (\omega_k + u_3)M_4 + (\omega_\nu + u_4)M_4\\
&\quad +(\alpha_{k\nu} + u_5)M_4 + (\mu + \eta_{k\nu})M_4 - \xi_\nu(\omega_\nu + u_4)M_5 - \xi_k(\omega_k + u_3)M_6 - \eta_{k\nu} M_7 - \gamma_3 M_8\\
&\quad -\tau_3 M_9 - (\alpha_{k\nu} + u_5)M_{10},\\
\frac{dM_5}{dt} &= -b_4 + (1-u_2)\varpi_\nu P_\nu M_5 + (\rho_k + u_3)M_5 + (\mu + \delta_k)M_5 - (1-u_2)\varpi_\nu P_\nu M_7 - \gamma_2 M_8\\
&\quad -(\rho_k + u_3)M_{10},\\
\frac{dM_6}{dt} &= -b_5 + (1-u_1)\varpi_k P_k M_6 + (\rho_\nu + u_4)M_6 + (\mu + \delta_\nu)M_6 - (1-u_1)\varpi_k P_k M_7 - \tau_2 M_9\\
&\quad -(\rho_\nu + u_4)M_{10},\\
\frac{dM_7}{dt} &= -b_6 - (\pi_\nu + u_4)M_5 - (\pi_k + u_3)M_6 + (\pi_k + u_3)M_7 + (\pi_\nu + u_4)M_7 + (\rho_{k\nu} + u_5)M_7\\
&\quad +(\mu + \delta_k + \delta_\nu)M_7 - \gamma_4 M_8 - \tau_4 M_9 - (\rho_{k\nu} + u_5)M_{10},\\
\frac{dM_8}{dt} &= -b_7 + (1-u_1)\varpi_k S M_1 - (1-u_1)\varpi_k S M_2 + (1-u_1)\varpi_k E_\nu M_3\\
&\quad -(1-u_1)(1-q_k)\varpi_k E_\nu M_4 + (1-u_1)\varpi_k I_\nu M_6 - (1-u_1)q_k \varpi_k E_\nu M_7\\
&\quad -(1-u_1)\varpi_k I_\nu M_7 + (\delta_1 + u_6)M_8,\\
\frac{dM_9}{dt} &= -b_8 + (1-u_2)\varpi_\nu S M_1 + (1-u_2)\varpi_\nu E_k M_2 - (1-u_2)\varpi_\nu S M_3
\end{aligned}$$

$$
\begin{aligned}
&-(1-u_2)(1-q_v)\varpi_v E_k M_4 + (1-u_2)\varpi_v I_k M_5 - (1-u_2)q_v\varpi_v E_k M_7\\
&-(1-u_2)\varpi_v I_k M_7 + (\delta_2+u_7)M_9,\\
\frac{dM_{10}}{dt} &= \mu M_{10}.
\end{aligned}
\tag{5.3}
$$

Proof. By the Pontryagin's maximum principle [21] and the Hamiltonian function (5.2), the adjoint system is computed by

$$
\frac{dM_1}{dt} = -\frac{\partial \mathcal{H}}{\partial S}, \quad \frac{dM_2}{dt} = -\frac{\partial \mathcal{H}}{\partial E_k}, \quad \frac{dM_3}{dt} = \frac{\partial \mathcal{H}}{\partial E_v}, \quad \frac{dM_4}{dt} = -\frac{\partial \mathcal{H}}{\partial E_{kv}}, \quad \frac{dM_5}{dt} = -\frac{\partial \mathcal{H}}{\partial I_k},
$$
$$
\frac{dM_6}{dt} = -\frac{\partial \mathcal{H}}{\partial I_v}, \quad \frac{dM_7}{dt} = -\frac{\partial \mathcal{H}}{\partial I_{kv}}, \quad \frac{dM_8}{dt} = -\frac{\partial \mathcal{H}}{\partial P_k}, \quad \frac{dM_9}{dt} = -\frac{\partial \mathcal{H}}{\partial P_v}, \quad \frac{dM_{10}}{dt} = -\frac{\partial \mathcal{H}}{\partial R}.
$$

These yield the following the adjoint system.

$$
\begin{aligned}
\frac{dM_1}{dt} &= (1-u_1)\varpi_k P_k M_1 + (1-u_2)\varpi_v P_v M_1 + \mu M_1 - (1-u_1)\varpi_k P_k M_2 - (1-u_2)\varpi_v P_v M_3,\\
\frac{dM_2}{dt} &= -b_1 + (\alpha_k+u_3)M_2 + ((1-u_2)\varpi_v P_v + \mu + \eta_k)M_2 - (1-u_2)(1-q_v)\varpi_v P_v M_4 - \eta_k M_5\\
&\quad -(1-u_2)q_v\varpi_v P_v M_7 - \gamma_1 M_8 - (\alpha_k+u_3)M_{10},\\
\frac{dM_3}{dt} &= -b_2 + (\alpha_v+u_4)M_3 + ((1-u_1)\varpi_k P_k + \mu + \eta_v)M_3 - (1-u_1)(1-q_k)\varpi_k P_k M_4 - \eta_v M_6\\
&\quad -(1-u_1)q_k\varpi_k P_k M_7 - \tau_1 M_9 - (\alpha_v+u_4)M_{10},\\
\frac{dM_4}{dt} &= -b_3 - (1-\xi_v)(\omega_v+u_4)M_2 - (1-\xi_k)(\omega_k+u_3)M_3 + (\omega_k+u_3)M_4 + (\omega_v+u_4)M_4\\
&\quad +(\alpha_{kv}+u_5)M_4 + (\mu+\eta_{kv})M_4 - \xi_v(\omega_v+u_4)M_5 - \xi_k(\omega_k+u_3)M_6 - \eta_{kv}M_7 - \gamma_3 M_8\\
&\quad -\tau_3 M_9 - (\alpha_{kv}+u_5)M_{10},\\
\frac{dM_5}{dt} &= -b_4 + (1-u_2)\varpi_v P_v M_5 + (\rho_k+u_3)M_5 + (\mu+\delta_k)M_5 - (1-u_2)\varpi_v P_v M_7 - \gamma_2 M_8\\
&\quad -(\rho_k+u_3)M_{10},\\
\frac{dM_6}{dt} &= -b_5 + (1-u_1)\varpi_k P_k M_6 + (\rho_v+u_4)M_6 + (\mu+\delta_v)M_6 - (1-u_1)\varpi_k P_k M_7 - \tau_2 M_9\\
&\quad -(\rho_v+u_4)M_{10},\\
\frac{dM_7}{dt} &= -b_6 - (\pi_v+u_4)M_5 - (\pi_k+u_3)M_6 + (\pi_k+u_3)M_7 + (\pi_v+u_4)M_7 + (\rho_{kv}+u_5)M_7\\
&\quad +(\mu+\delta_k+\delta_v)M_7 - \gamma_4 M_8 - \tau_4 M_9 - (\rho_{kv}+u_5)M_{10},\\
\frac{dM_8}{dt} &= -b_7 + (1-u_1)\varpi_k S M_1 - (1-u_1)\varpi_k S M_2 + (1-u_1)\varpi_k E_v M_3\\
&\quad -(1-u_1)(1-q_k)\varpi_k E_v M_4 + (1-u_1)\varpi_k I_v M_6 - (1-u_1)q_k\varpi_k E_v M_7\\
&\quad -(1-u_1)\varpi_k I_v M_7 + (\delta_1+u_6)M_8,\\
\frac{dM_9}{dt} &= -b_8 + (1-u_2)\varpi_v S M_1 + (1-u_2)\varpi_v E_k M_2 - (1-u_2)\varpi_v S M_3\\
&\quad -(1-u_2)(1-q_v)\varpi_v E_k M_4 + (1-u_2)\varpi_v I_k M_5 - (1-u_2)q_v\varpi_v E_k M_7\\
&\quad -(1-u_2)\varpi_v I_k M_7 + (\delta_2+u_7)M_9,\\
\frac{dM_{10}}{dt} &= \mu M_{10}.
\end{aligned}
\tag{5.4}
$$

Finding the partial derivatives of the Hamiltonian function (5.2) with respect to each control variable yields the optimality equations.

$$\left.\begin{aligned}
\frac{\partial \mathcal{H}}{\partial u_1} =& \varpi_k P_k S M_1 - \varpi_k P_k S M_2 + \varpi_k P_k E_v M_3 - (1-q_k)\varpi_k P_k E_v M_4 + \varpi_k P_k I_v M_6 \\
& - q_k \varpi_k P_k E_v M_7 - \varpi_k P_k I v M_7 + \nu_1 u_1, \\
\frac{\partial \mathcal{H}}{\partial u_2} =& \varpi_v P_v S M_1 - \varpi_v P_v S M_3 + \varpi_v P_v E_k M_2 - (1-q_v)\varpi_v P_v E_k M_4 + \varpi_v P_v I_k M_5 \\
& - q_v \varpi_v P_v E_k M_7 - \varpi_v P_v I k M_7 + \nu_2 u_2, \\
\frac{\partial \mathcal{H}}{\partial u_3} =& - E_k M_2 + (1-\xi_k) E_{kv} M_3 - E_{kv} M_4 - I_k M_5 + \xi_k E_{kv} M_6 + I_{kv} M_6 - I_{kv} M_7 + E_k M_{10} \\
& + I_k M_{10} + \nu_3 u_3, \\
\frac{\partial \mathcal{H}}{\partial u_4} =& - E_v M_3 + (1-\xi_v) E_{kv} M_2 - E_{kv} M_4 + \xi_v E_{kv} M_5 - I_v M_6 + I_{kv} M_5 - I_{kv} M_7 + E_v M_{10} \\
& + I_v M_{10} + \nu_4 u_4, \\
\frac{\partial \mathcal{H}}{\partial u_5} =& - E_{kv} M_4 + E_{kv} M_{10} - I_{kv} M_7 + I_{kv} M_{10} + \nu_5 u_5, \\
\frac{\partial \mathcal{H}}{\partial u_6} =& - P_k M_8 + \nu_6 u_6, \\
\frac{\partial \mathcal{H}}{\partial u_7} =& - P_v M_9 + \nu_7 u_7.
\end{aligned}\right\} \tag{5.5}$$

To obtain optimal controls u_i^* ($i = 1,\ 2, \cdots, 7$), we replace u_i in the system (5.5) with $\bar{u}_i$ and equate the right-hand side of the equations of the resulting system to zero then solve for $\bar{u}_i$. Thus, we get

$$\begin{aligned}
\bar{u}_1 =& \frac{\varpi_k P_k(-SM_1 + SM_2 - E_v M_3 + (1-q_k)E_v M_4 - I_v M_6 + q_k E_v M_7 + I_v M_7)}{\nu_1}, \\
\bar{u}_2 =& \frac{\varpi_v P_v(-SM_1 + SM_3 - E_k M_2 + (1-q_v)E_k M_4 - I_k M_5 + q_v E_k M_7 + I_k M_7)}{\nu_2} \\
\bar{u}_3 =& \frac{E_k M_2 - (1-\xi_k)E_{kv} M_3 + E_{kv} M_4 + I_k M_5 - \xi_k E_{kv} M_6 - I_{kv} M_6 + I_{kv} M_7 - E_k M_{10} - I_k M_{10}}{\nu_3}, \\
\bar{u}_4 =& \frac{E_v M_3 - (1-\xi_v)E_{kv} M_2 + E_{kv} M_4 - \xi_v E_{kv} M_5 + I_v M_6 - I_{kv} M_5 + I_{kv} M_7 - E_v M_{10} - I_v M_{10}}{\nu_4}, \\
\bar{u}_5 =& \frac{E_{kv} M_4 - E_{kv} M_{10} + I_{kv} M_7 - I_{kv} M_{10}}{\nu_5}, \\
\bar{u}_6 =& \frac{P_k M_8}{\nu_6}, \\
\bar{u}_7 =& \frac{P_v M_9}{\nu_7}.
\end{aligned}$$

Using the standard control arguments that involve the bounds of the controls, we come to

the following conclusion:

$$u_i^* = \begin{cases} 0 & \text{if } \bar{u}_i \leqslant 0, \\ \bar{u}_i & \text{if } 0 < \bar{u}_i < 1, \\ 1 & \text{if } \bar{u}_i \geqslant 1, \end{cases} \tag{5.6}$$

In compact notation, the system (5.6) can be written as

$$\left.\begin{aligned} u_1^* &= \max\{0, \min\{1, \bar{u}_1\}\}, & u_5^* &= \max\{0, \min\{1, \bar{u}_5\}\}, \\ u_2^* &= \max\{0, \min\{1, \bar{u}_2\}\}, & u_6^* &= \max\{0, \min\{1, \bar{u}_6\}\}, \\ u_3^* &= \max\{0, \min\{1, \bar{u}_3\}\}, & u_7^* &= \max\{0, \min\{1, \bar{u}_7\}\}. \\ u_4^* &= \max\{0, \min\{1, \bar{u}_4\}\}, \end{aligned}\right\} \tag{5.7}$$

□

6. Numerical Simulation

Analytical solutions to the optimality system may not always be feasible; in these cases, numerical approaches are employed to approximate the solutions and illustrate the results. The optimality system, which consists of the state system (2.1), adjoint system (5.4), control characterization (5.7), and corresponding initial conditions, is solved iteratively to produce the numerical simulation results shown in this section. The fourth-order Runge-Kutta algorithm is used to solve the state and adjoint equations using the parameter values in Table (1).

Table 1: Parameter values

Parameter	Value	Source	Parameter	Value	Source
Λ	0.00133	[22]	η_v	0.05	Assumed
ϖ_k	0.0007954551	Assumed	η_{kv}	0.01	Assumed
ϖ_v	0.000209819	Assumed	ρ_k	0.005	Assumed
μ	0.00056	[22]	ρ_v	0.0433	Assumed
δ_k	0.0001	Assumed	ρ_{kv}	0.0052	Assumed
δ_v	0.01	Assumed	α_k	0.001	Assumed
δ_1	0.0900982	Assumed	α_v	0.001	Assumed
δ_2	0.19009821	Assumed	α_{kv}	0.013	Assumed
q_k	0.3	Assumed	γ_1	0.0587365	Assumed
q_v	0.3	Assumed	γ_2	0.0487364	Assumed
ξ_k	0.00911	Assumed	γ_3	0.0091	Assumed
ξ_v	0.009	Assumed	γ_4	0.00921	Assumed
ω_k	0.09	Assumed	τ_1	0.1	Assumed
ω_v	0.08	Assumed	τ_2	0.1	Assumed
π_k	0.004	Assumed	τ_3	0.191	Assumed
π_v	0.0039	Assumed	τ_4	0.12	Assumed
η_k	0.01	Assumed			

The optimal strategy for considerably reducing the spread of the CBD-CLR co-infection is investigated among the following control strategies:

(i) Control with prevention of CBD and CLR infections (u_1, u_2)

(ii) Control with Treatment of CBD, CLR and CBD-CLR co-infection (u_3, u_4, u_5)

(iii) Control with elimination of *Colletotrichum kahawae* and *Hemileia vastatrix* pathogens (u_6, u_7)

(iv) Control with prevention of CBD and CLR infections and Treatment of CBD, CLR and CBD-CLR co-infection (u_1, u_2, u_3, u_4, u_5)

(v) Control with prevention of CBD and CLR infections and elimination of *Colletotrichum kahawae* and *Hemileia vastatrix* pathogens (u_1, u_2, u_6, u_7)

(vi) Control with Treatment of CBD, CLR and CBD-CLR co-infection and elimination of *Colletotrichum kahawae* and *Hemileia vastatrix* pathogens (u_3, u_4, u_5, u_6, u_7)

(vii) Using all interventions (u_1, u_2, u_3, u_4, u_5, u_6, u_7)

For the simulation of the model with optimal control, we made the following assumptions: $b_1 = 5$, $b_2 = 4$, $b_3 = 9$, $b_4 = 6$, $b_5 = 6$, $b_6 = 11$, $b_7 = 6$, $b_8 = 5$, $\nu_1 = 100$, $\nu_2 = 100$, $\nu_3 = 100$, $\nu_4 = 100$, $\nu_5 =$, $\nu_6 = 100$ and $\nu_7 = 100$. In addition, we utilized the initial: $S_0 = 10000$, $E_{k0} = 500$, $E_{\nu 0} = 101$, $E_{k\nu 0} = 2002$, $I_{k0} = 100$, $I_{\nu 0} = 10$, $I_{k\nu 0} = 12$, $P_{k0} = 1600$, $P_{\nu 0} = 1601$, and $R_0 = 10$

6.1. Numerical Simulation Results and Discussion

6.1.1. Strategy 1: Control with prevention of CBD and CLR infections (u_1, u_2)

In this strategy, the objective function $\mathcal{J}$ is optimized using both prevention of CBD infection u_1 and prevention of CLR infection u_2 while other interventions (u_3, u_4, u_5, u_6, u_7) are set to zero. In Figure 2(a), it is seen that prevention has a significant impact on controlling the emergence of new infection cases of CBD and CLR infections since the solution curve of the susceptible coffee plants S(t) without control converges to the lower bound at a higher rate than that with controls. From Figures 2(d), 2(g), 2(h) and 2(i) we observed a positive effect of prevention since the solution curves of the co-exposed coffee plants $E_{k\nu}(t)$, the co-infected coffee plants $I_{k\nu}(t)$, *Colletotrichum kahawae* pathogens $P_k(t)$ and *Hemileia vastatrix* pathogens $P_\nu(t)$ without control continue rising and those with controls converge to the lower bound. This implies that prevention alone is effective in reducing co-infected coffee plants $I_{k\nu}(t)$, *Colletotrichum kahawae* pathogens $P_k(t)$ and *Hemileia vastatrix* pathogens $P_\nu(t)$ as result of reduced new infection cases which in turn lead reduced shedding of pathogens. The effect of this strategy is observed in Figures 2(b) and 2(c), where the solution curves with control rise steadily to certain levels which are lower than the peaks of the solution curves without control and start falling to the lower bound. We also noticed a steady increase in the number of infection cases of CBD-infected coffee plants $I_k(t)$, the CLR-infected coffee plants $I_\nu(t)$ in Figure 2(e) and Figure 2(f) respectively, implying that this strategy is not effective in controlling infected coffee plants in $I_k(t)$ and $I_\nu(t)$ compartments. This can be related to the lack of control measures, such as treatment in these compartments.

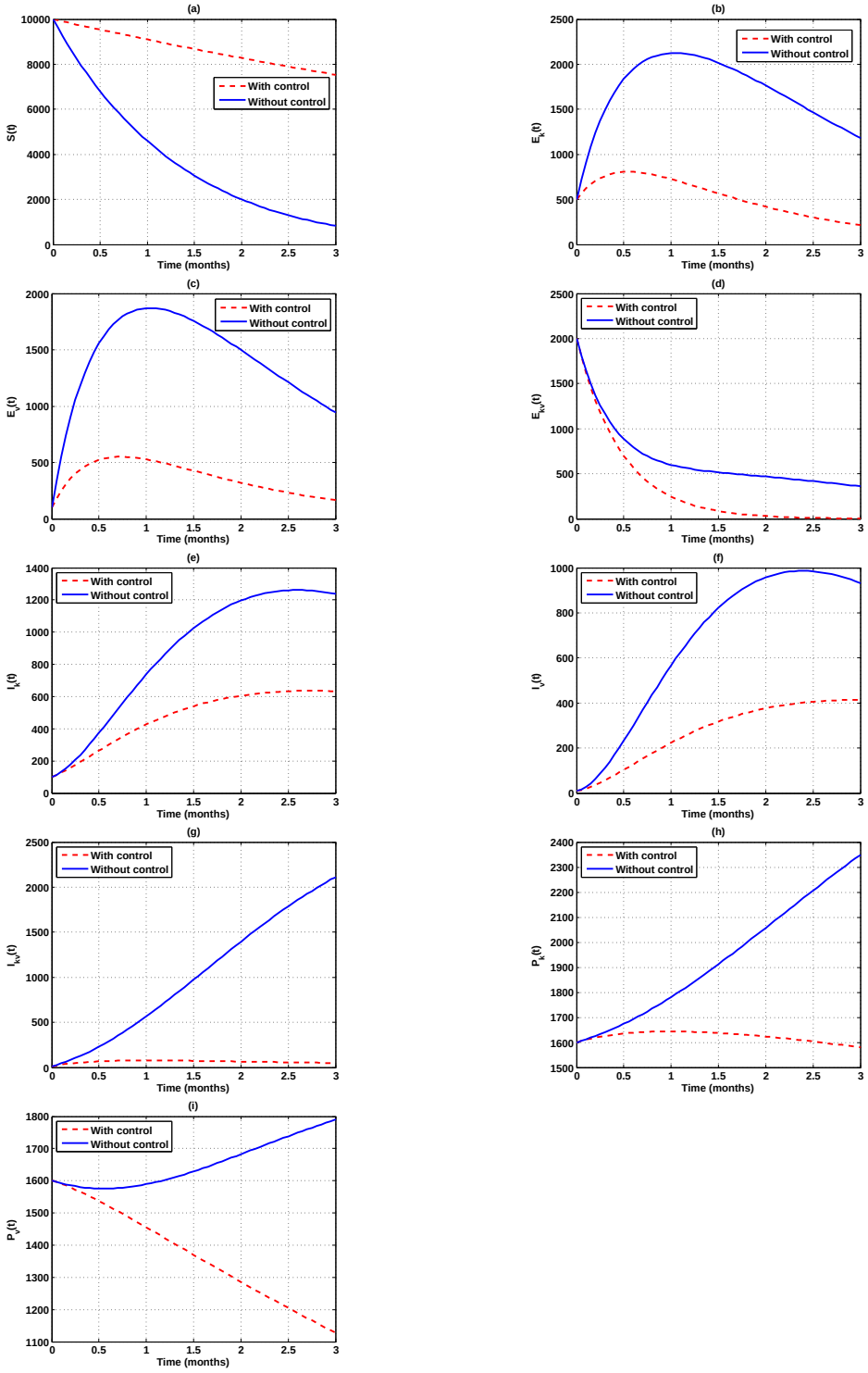

Figure 2: Graphs showing the effect of prevention of CBD and CLR infections (u_1, u_2) on CBD and CLR co-infection model

6.1.2. Strategy 2: Control with treatment of CBD, CLR and CBD-CLR co-infection (u_3, u_4, u_5)

In this strategy, the objective function $\mathcal{J}$ is optimized using both treatment of CBD infection u_3, CLR infection u_4 and CBD-CLR co-infection u_5 while other interventions (u_1, u_2, u_6, u_7) are set to zero. In Figure 3(a), we observed the solution curves of the susceptible coffee plants S(t) without controls and that of the susceptible coffee plants S(t) with controls; they almost converge to zero at the same rate whereby the S(t) with controls is slightly above that of S(t) without controls. This implies that this strategy is inefficient in reducing new CBD and CLR infection cases. From Figures 3(d) and 3(i), we observed a continuous decrease in numbers in the solution curves with controls. This may be connected to the effectiveness of the strategy. In Figures 3(b), 3(c), 3(e), 3(f), 3(g) and 3(h), we noticed a slight rise of solution curves with controls to a level below that of curves without controls and followed by a steady decrease hence converging to zero. This suggests that strategy 2 effectively controls the cases at the end of the given period but not at the beginning in six compartments.

6.1.3. Strategy 3: Control with elimination of Colletotrichum kahawae and Hemileia vastatrix pathogens (u_6, u_7)

In this strategy, the objective function $\mathcal{J}$ is optimized by using the elimination of *Colletotrichum kahawae* pathogens u_6 and *Hemileia vastatrix* pathogens u_7. At the same time, other interventions are set to zero. The impact of eliminating pathogens is noticed in Figure 4(a) since the rate at which the solution curve with controls converges to zero is lower than that of the curve without control. Hence, this strategy can be used to reduce cases. Figures 4(d), 4(h) and 4(i) demonstrate that this strategy is effective in reducing the co-exposed coffee plants, *Colletotrichum kahawae* pathogens and *Hemileia vastatrix* pathogens respectively. Figures 4(b), 4(c) and 4(g) have shown that this strategy cannot contain the infections at the onset of the disease since the curves rise first and then fall. Also, from Figures 4(e) and 4(f), we observed that this strategy is completely not effective in reducing the CBD-infected coffee plants $I_k(t)$ and the CLR-infected coffee plants $I_v(t)$ since their solution curves continue rising.

6.1.4. Strategy 4: Control with prevention of CBD and CLR infections and Treatment of CBD, CLR and CBD-CLR co-infection (u_1, u_2, u_3, u_4, u_5)

Prevention of CBD and CLR infections and Treatment of CBD, CLR, and CBD-CLR co-infection (u_1, u_2, u_3, u_4, u_5) are used to optimize the objective function $\mathcal{J}$ while u_6 and u_7 are set equal to zero. In Figures 5(a), we observed that this strategy has a positive impact on controlling the emergence of new infection cases of CBD and CLR infections since the solution curve of the susceptible coffee plants S(t) with control converges to zero at a lower rate. We observed positive results in Figures 5(d), 5(g), 5(h) and 5(i) since the solution curves with controls steadily converge to zero. From Figures 5(b), 5(c), 5(e) and 5(f), we observed a slight increase of cases for the solution curves with controls at the beginning of a given infection period followed by a decrease which converges to zero. This suggests that this strategy effectively controls infection cases since the cases increase slightly and eventually converge to zero.

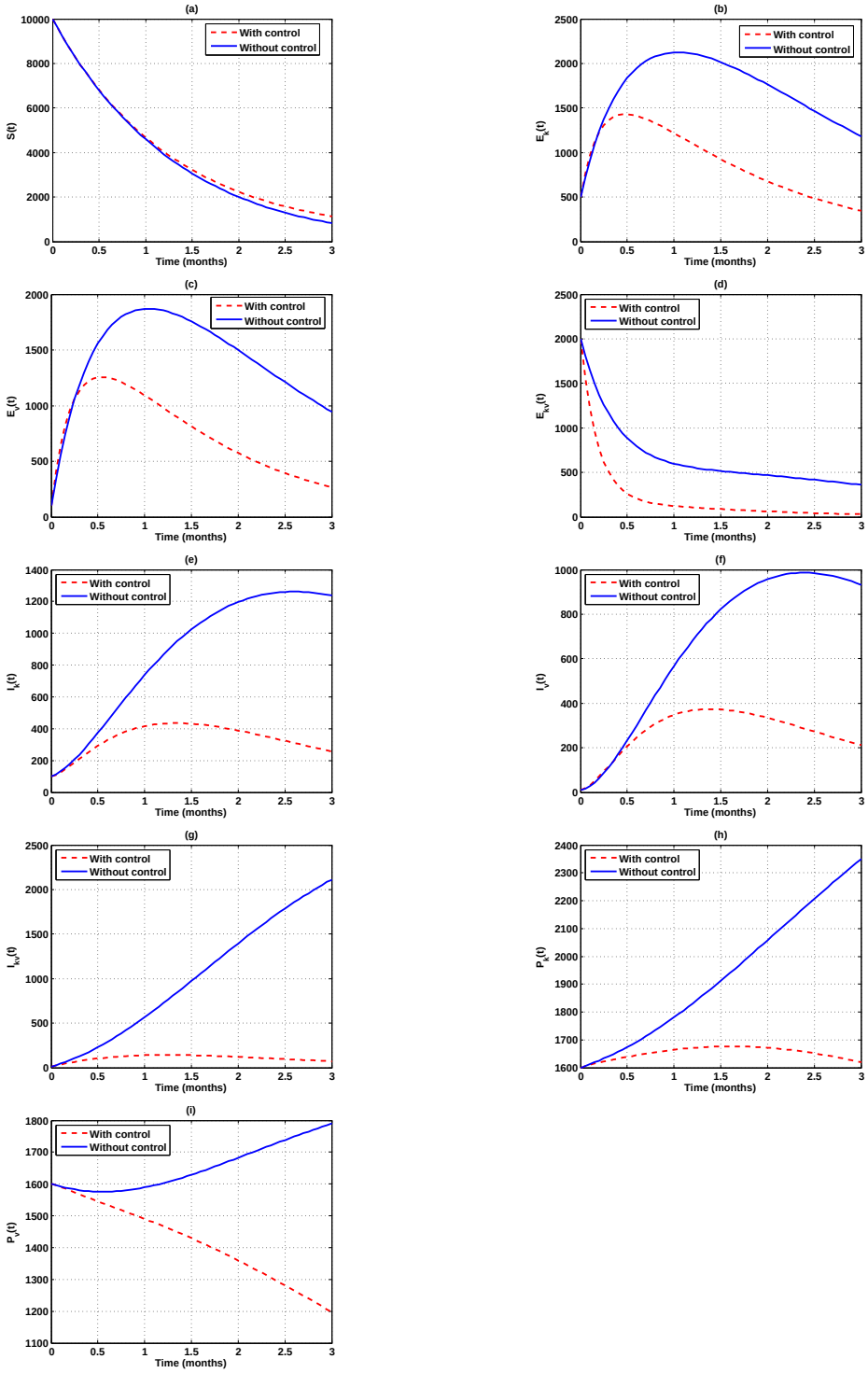

Figure 3: Graphs effect of treatment of CBD, CLR, and CBD-CLR co-infection (u_3, u_4, u_5) on CBD and CLR co-infection model

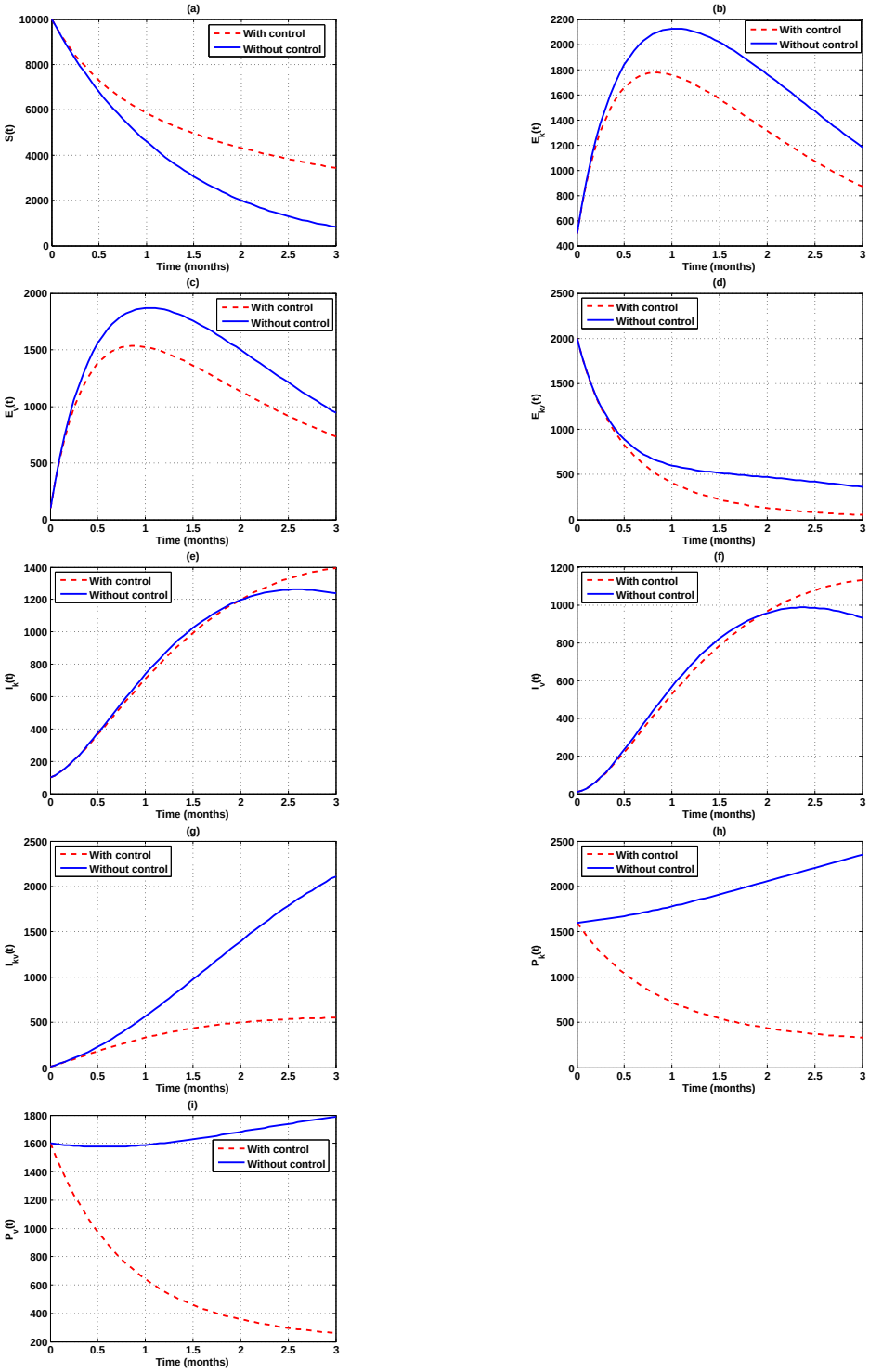

Figure 4: Graphs showing the elimination of *Colletotrichum kahawae* and *Hemileia vastatrix* pathogens (u_6, u_7)

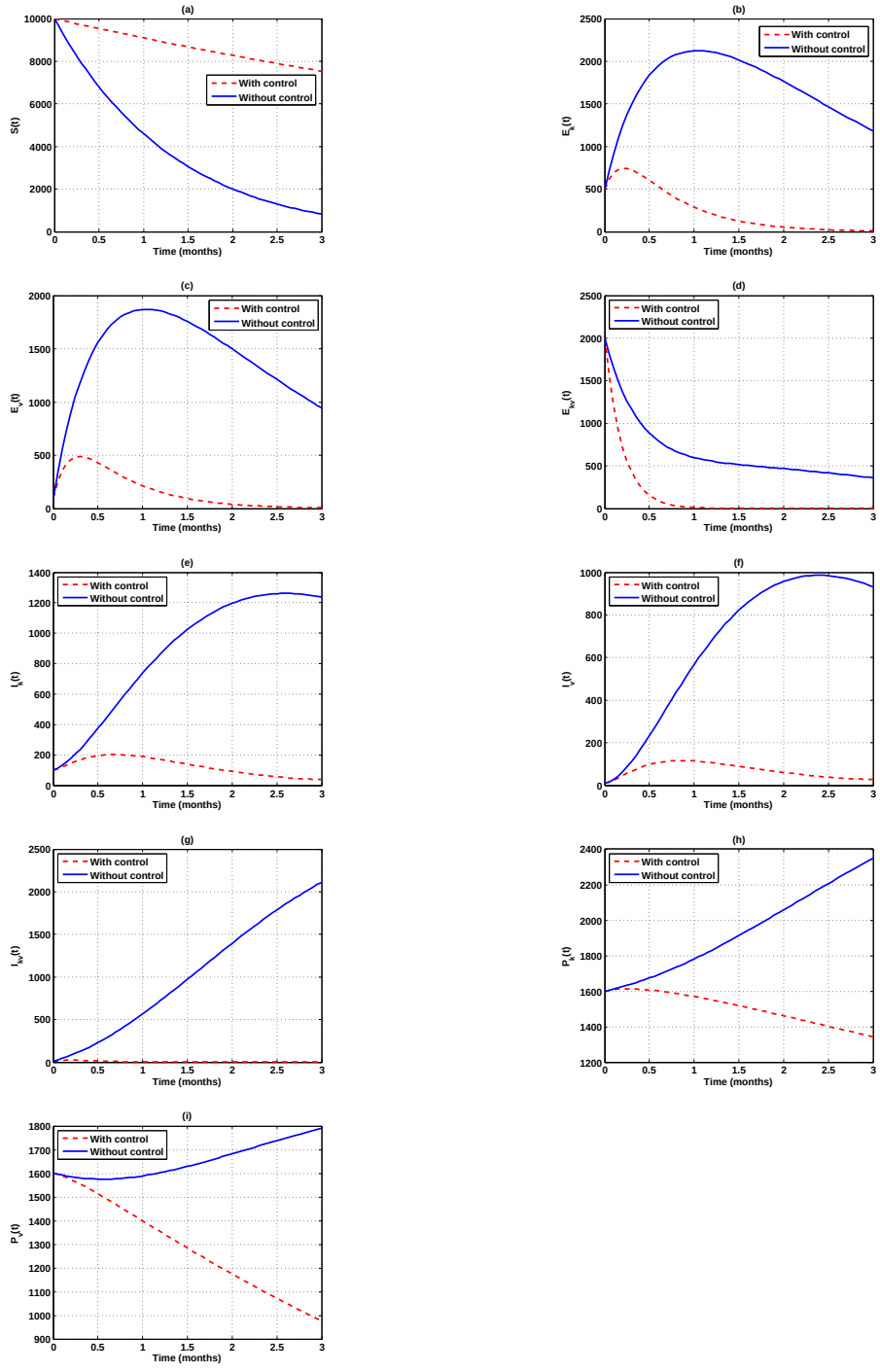

Figure 5: Graphs showing the effect of prevention of CBD and CLR infections and Treatment of CBD, CLR, and CBD-CLR co-infection (u_1, u_2, u_3, u_4, u_5) on CBD and CLR co-infection model

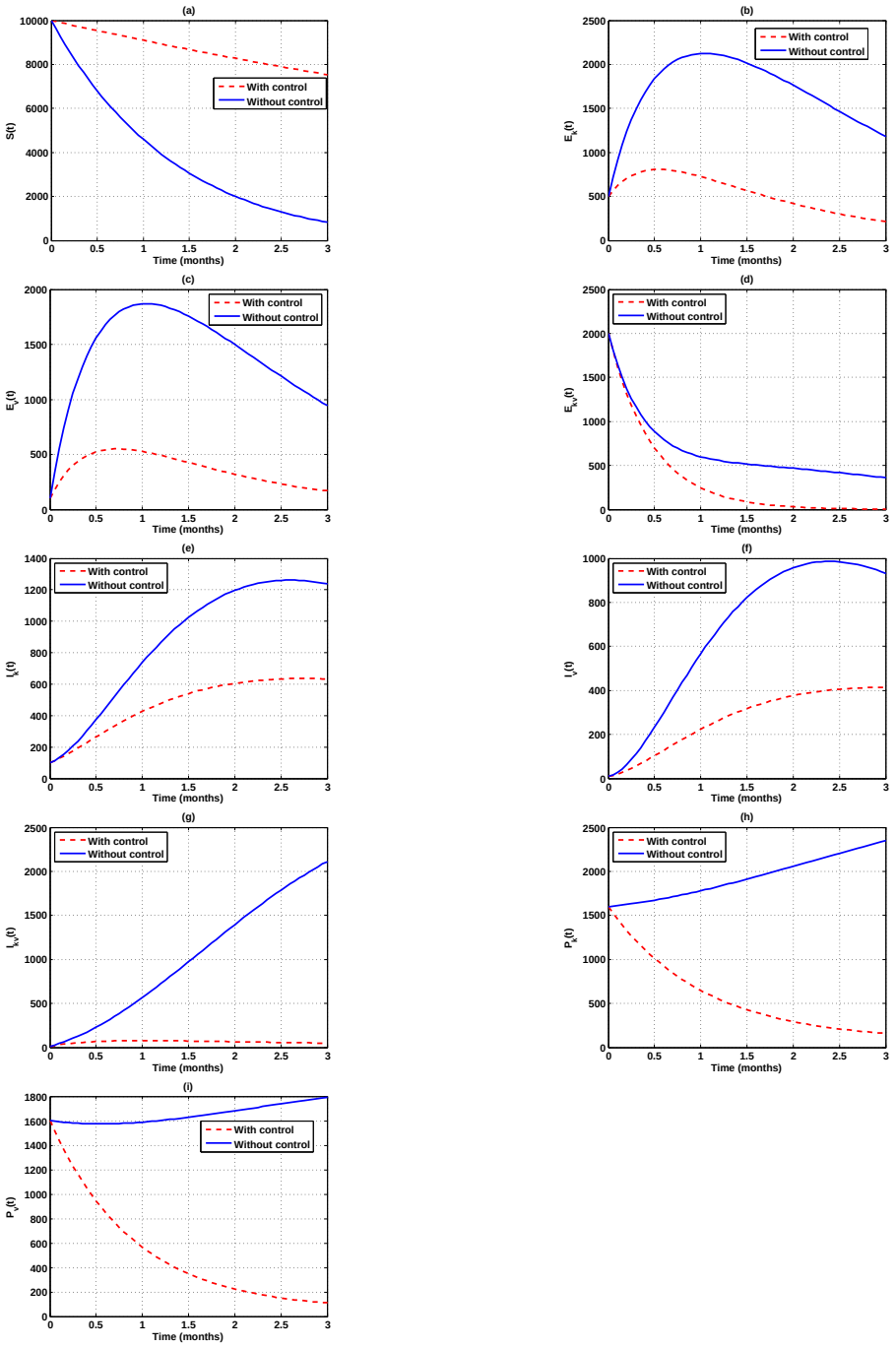

Figure 6: Graphs showing the effect of prevention of CBD and CLR infections and elimination of *Colletotrichum kahawae* and *Hemileia vastatrix* pathogens (u_1, u_2, u_6, u_7) on CBD and CLR co-infection model

6.1.5. Strategy 5: Control with prevention of CBD and CLR infections and elimination of Colletotrichum kahawae and Hemileia vastatrix pathogens (u_1, u_2, u_6, u_7)

Prevention of CBD and CLR infections and elimination of *Colletotrichum kahawae* and *Hemileia vastatrix* pathogens (u_1, u_2, u_6, u_7) are used to optimize the objective function $\mathcal{J}$ while (u_3, u_4, u_5) are set to zero. We observed positive results in Figure 6(a) since this strategy significantly reduced the number of new infection cases. We also observed positive results in Figures 6(d), 6(g), 6(h) and 6(i) since this strategy is effective in reducing the numbers of the co-exposed coffee plants $E_{kv}(t)$, the co-infected coffee plants $I_{kv}(t)$, *Colletotrichum kahawae* pathogens $P_k(t)$ and *Hemileia vastatrix* pathogens $P_v(t)$ respectively. In Figures 6(b), 6(c), 6(e) and 6(f), we noticed an increase of cases for the solution curves with controls at the beginning of a given period followed by a decrease.

6.1.6. Strategy 6: Control with the treatment of CBD, CLR and CBD-CLR co-infection and elimination of Colletotrichum kahawae and Hemileia vastatrix pathogens (u_3, u_4, u_5, u_6, u_7)

In this strategy, treatment of CBD, CLR and CBD-CLR co-infection and elimination of *Colletotrichum kahawae* and *Hemileia vastatrix* pathogens (u_3, u_4, u_5, u_6, u_7) are used to optimize the objective function $\mathcal{J}$ while (u_1, u_2 are set to zero. From Figure 7(a), we noticed that this strategy is moderately able to reduce the number of new infection cases since the solution curve of S(t) with controls is slightly above that of S(t) without controls. This is connected to treating CBD, CLR, and CBD-CLR co-infection and eliminating pathogens. We noted positive results in Figures 7(d), 7(g), 7(h) and 7(i) since the solution curves with controls steadily converge to zero. In Figures 7(b), 7(c), 7(e) and 7(f), we observed that the solution curves with controls rise to certain levels then fall as they converge to zero. This suggests that this strategy is not effective in controlling the cases at the beginning of a given infection period.

6.1.7. Strategy 7: Using all interventions (u_1, u_2, u_3, u_4, u_5, u_6, u_7)

The objective function $\mathcal{J}$ is optimized using all control mechanisms (u_1, u_2, u_3, u_4, u_5, u_6, u_7) in this strategy. We observed that Figures 8(a), 8(b), 8(c), 8(d), 8(e), 8(f), 8(g) are similar to the corresponding figures in Figure 5. This suggests that the effectiveness of strategies 4 and 7 is almost the same. The only difference is that Figures 8(h) and 8(i) are not similar to the corresponding figures in Figure 5. This is because the solution curves with controls in Figures 8(h) and 8(i), converge to zero at a higher rate than those of Figures 5(h) and 5(i). This suggests that strategy 7 is more effective in reducing the pathogens than strategy 4.

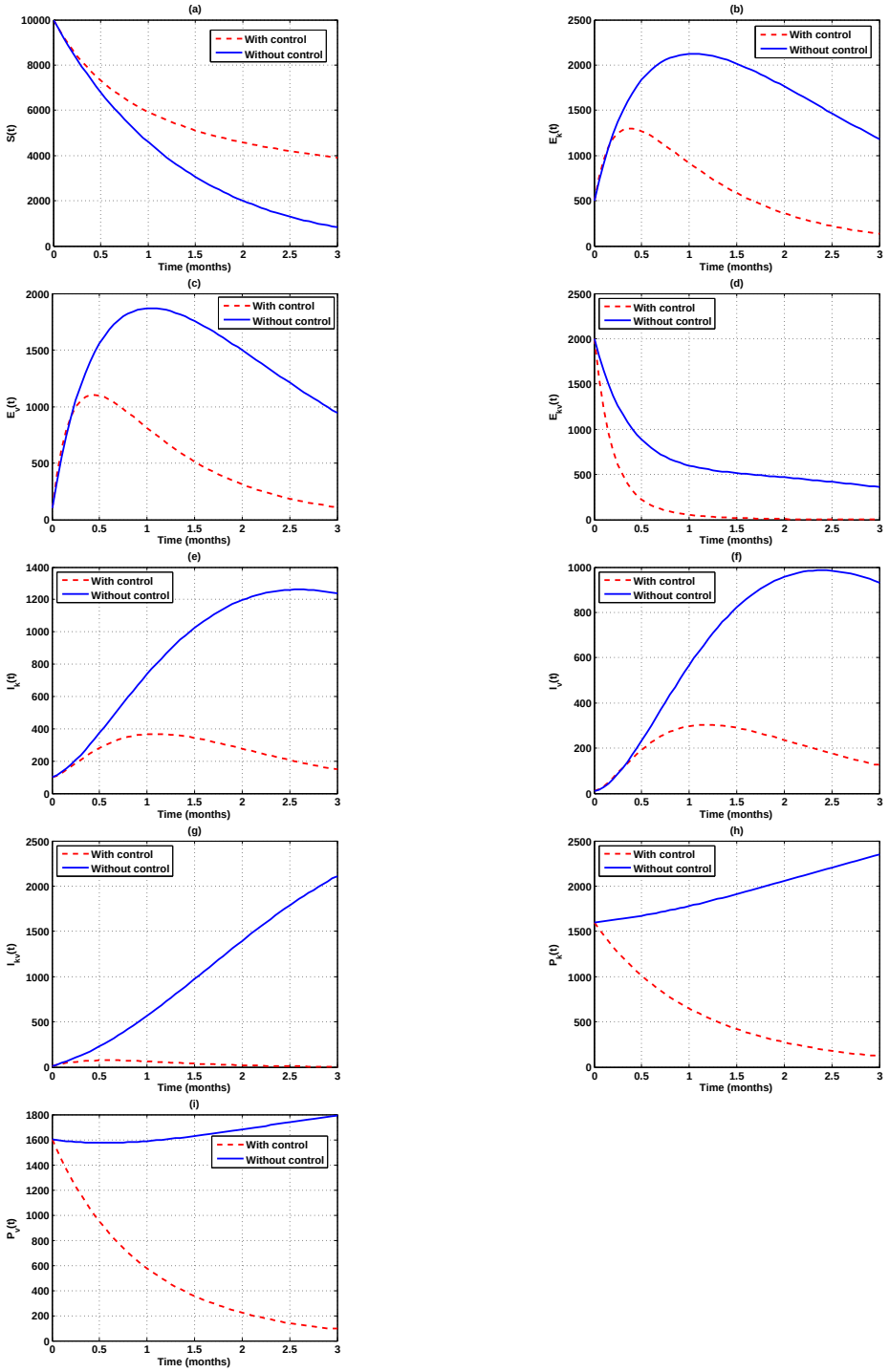

Figure 7: Graphs showing the effect of treatment of CBD, CLR and CBD-CLR co-infection and elimination of *Colletotrichum kahawae* and *Hemileia vastatrix* pathogens (u_3, u_4, u_5, u_6, u_7) on CBD and CLR co-infection model

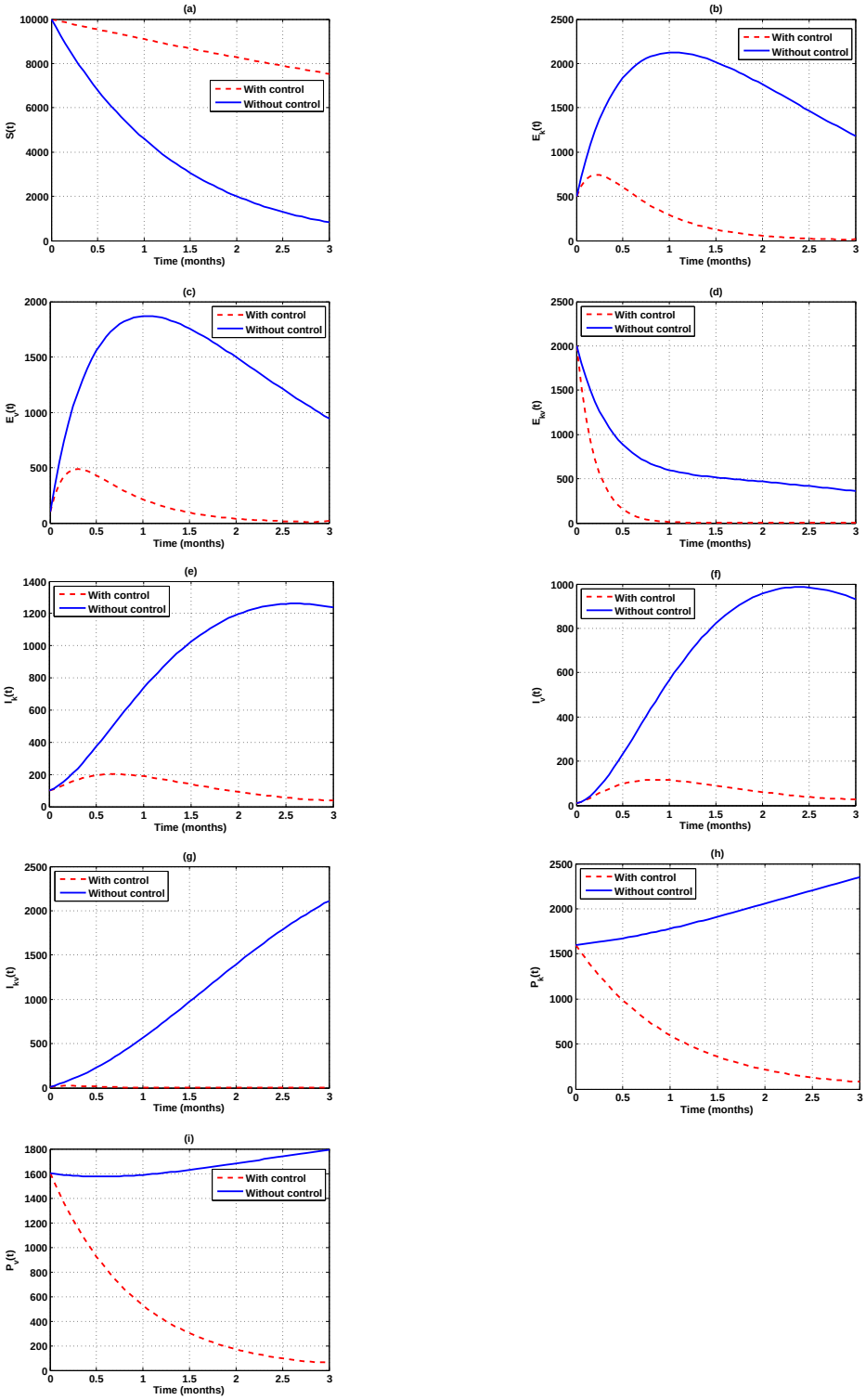

Figure 8: Graphs showing the effect of all interventions (u_1, u_2, u_3, u_4, u_5, u_6, u_7) on CBD and CLR co-infection model

7. Conclusion

This paper develops a mathematical model for the co-infection of CBD and CLR with the prevention of CBD infection, prevention of CLR infection, the treatment of CBD-infected coffee plants, the treatment of CLR-infected coffee plants, the treatment of CBD-CLR Co-infected coffee plants, elimination of *Colletotrichum kahawae* pathogens and elimination of *Hemileia vastatrix* pathogens. The model's qualitative examination reveals that its solution is bounded and positive. The optimal control problem is formulated using Pontryagin's maximum principle, and the conditions for optimal disease control are analyzed. The optimality system is created, and existence requirements for optimal control are identified. The elimination of CBD-CLR co-infection is recommended using seven strategies, with each strategy's effectiveness being examined. The recommended strategies are numerically examined, and the outcomes are graphically presented. The outcomes indicate that combining all interventions is the best strategy for slowing the spread of the CBD-CLR co-infection.

Acknowledgement

The authors appreciate the ample time given by their respective universities towards this manuscript.

References

[1] Coffee production in Kenya. Retrieved May 13, 2021, from http://www.ico.org/documents/cy2018-19/icc-124-7e-profile-kenya.pdf

[2] Condliffe K, Kebuchi W, Love C, and Ruparell R, (2008)"Kenya coffee: a cluster analysis" *Professor Michael Porter, Microeconomics of Competitiveness. Harvard Business School*, 2.

[3] McDonald J (1926)."A preliminary account of a disease of green coffee berries in Kenya," *Transactions of the British Mycological Society*. 11 (1–2): 145–154. doi:10.1016/S0007-1536(26)80033-6

[4] Gichuru EK, Ithiru JM, Silva MC, Pereira A P and Varzea VM (2012)."Additional physiological races of coffee leaf rust (Hemileia vastatrix) identified in Kenya," *Tropical Plant Pathology*, 37(6), 424-427. doi.org/10.1590/S1982-56762012000600008

[5] Gichuru E, Alwora G, Gimase J, Kathurima C. (2021)."Coffee leaf rust (Hemileia vastatrix) in Kenya—A review." *Agronomy*. 20;11(12):2590. doi.org/10.3390/agronomy11122590

[6] Alworah G and Gichuru E, (2014)." Advances in the Management of Coffee Berry Disease and Coffee Leaf Rust in Kenya," *Journal of Renewable Agriculture* 2(1):5. doi:10.12966/jra.03.02.2014

[7] Nannyonga B, Luboobi L Tushemerirwe P and Jabłońska-Sabuka M (2015). "Using contaminated tools fuels outbreaks of Banana Xanthomonas Wilt: An optimal control study within-plantations using Runge-Kutta 4th order algorithms," *International Journal of Biomathematics*, 8(05), 1550065. doi.org/10.1142/S1793524515500655

[8] Abdo, M. S., Kamarany, M. A. A., Suhail, K. A., & Majam, A. S. (2022). Vaccination-based Measles Outbreak Model with Fractional Dynamics. Abhath Journal of Basic and Applied Sciences, 1(2), 6-10. doi.org/10.59846/ajbas.v1i2.439

[9] Sadek, L., Sadek, O., Alaoui, H. T., Abdo, M. S., Shah, K., & Abdeljawad, T. (2023). Fractional order modeling of predicting COVID-19 with isolation and vaccination strategies in Morocco. CMES-Comput. Model. Eng. Sci, 136, 1931-1950. doi:10.32604/cmes.2023.025033

[10] Nyaberi HO, Mutuku WN, Malonza DM and Gachigua GW (2023)." A Mathematical Model of the Dynamics of Coffee Berry Disease," Journal of Applied Mathematics. doi.org/10.1155/2023/9320795

[11] Avelino J, Zelaya H, Merlo A, Pineda A, Ordóñez M and Savary S (2006). "The intensity of a coffee rust epidemic is dependent on production situations," *Ecological modelling*, 197(3-4), 431-447. doi.org/10.1016/j.ecolmodel.2006.03.013

[12] Vandermeer J and Rohani P (2014).“The interaction of regional and local in the dynamics of the coffee rust disease," *arXiv preprint arXiv*:1407.8247. doi.org/10.48550/arXiv.1407.8247

[13] Vandermeer J, Hajian-Forooshani Z, and Perfecto I, (2018).“The dynamics of the coffee rust disease: an epidemiological approach using network theory" *European journal of plant pathology*, 150(4), 1001-1010. doi.org/10.1007/s10658-017-1339-x

[14] Djuikem C, Grognard F, Wafo RT, Touzeau S, and Bowong S, (2021).“Modelling coffee leaf rust dynamics to control its spread," Mathematical Modelling of Natural Phenomena, 16, 26. doi.org/10.1051/mmnp/2021018

[15] Djuikem C, Yabo AG, Grognard F, and Touzeau S, (2021). “ Mathematical modelling and optimal control of the seasonal coffee leaf rust propagation," *IFAC-PapersOnLine*, 54(5), 193-198. https://doi.org/10.1016/j.ifacol.2021.08.497

[16] Roeger LI, Feng Z, and Castillo-Chavez C, (2009). “Modeling TB and HIV co-infections," *Mathematical biosciences and engineering* : MBE, 6(4), 815–837. https://doi.org/10.3934/mbe.2009.6.815

[17] Nthiiri JK, Lawi GO, and Manyonge A (2015).“Mathematical modelling of tuberculosis as an opportunistic respiratory co-infection in HIV / AIDS in the presence of protection," *Appl. Math. Sci*. 9(105): 5215–5233. doi.org/10.12988/ams.2015.54365

[18] Okosun KO, and Makinde OD (2014). “A co-infection model of malaria and cholera diseases with optimal control”' *Mathematical Biosciences*, 258, 19-32, ISSN 0025-5564. https://doi.org/10.1016/j.mbs.2014.09.008

[19] Getachew TT, Oluwole DM and Malonza D (2018). “Co-dynamics of Pneumonia and Typhoid fever diseases with cost-effective optimal control analysis," *Applied Mathematics and Computation*, 316, 438-459, 0096-3003. https://doi.org/10.1016/j.amc.2017.07.063

[20] Anco DJ (2018).“Continuing consideration of co-infection and multiple pests," *APS Features*. doi:10.1094/APSFeature-2018-4

[21] Pontryagin LS, Boltyanskii VG, Gamkrelidze RV and Mishchenko EF (1962). *The Mathematical Theory of Optimal Processes*, Interscience Publishers, John Wiley, New York. https://doi.org/10.1002/zamm.19630431023

[22] Muhumuza C (2018). A mathematical model for the transmission dynamics and optimal control strategy of Coffee Wilt disease (Doctoral dissertation), Makerere University. http://hdl.handle.net/10570/6816